Swift observations of the 2015 outburst of AG Peg – from slow nova to classical symbiotic outburst

Gavin Ramsay,[1]★ J. L. Sokoloski,[2] G. J. M. Luna[3] and N. E. Nuñez[4]

[1]*Armagh Observatory, College Hill, Armagh BT61 9DG, UK*
[2]*Columbia Astrophysics Lab, 550 W120th St., 1027 Pupin Hall, MC 5247 Columbia University, NY 10027, USA*
[3]*Instituto de Astronomía y Física del Espacio (IAFE, CONICET-UBA), Av. Inte. Güiraldes 2620, C1428ZAA, Buenos Aires, Argentina*
[4]*Instituto de Ciencias Astronómicas de la Tierra y el Espacio (ICATE-UNSJ), Av. Espanã (sur) 1512, 5400 San Juan, Argentina*

ABSTRACT

Symbiotic stars often contain white dwarfs with quasi-steady shell burning on their surfaces. However, in most symbiotics, the origin of this burning is unclear. In symbiotic slow novae, however, it is linked to a past thermonuclear runaway. In 2015 June, the symbiotic slow nova AG Peg was seen in only its second optical outburst since 1850. This recent outburst was of much shorter duration and lower amplitude than the earlier eruption, and it contained multiple peaks – like outbursts in classical symbiotic stars such as Z And. We report *Swift* X-ray and UV observations of AG Peg made between 2015 June and 2016 January. The X-ray flux was markedly variable on a time-scale of days, particularly during four days near optical maximum, when the X-rays became bright and soft. This strong X-ray variability continued for another month, after which the X-rays hardened as the optical flux declined. The UV flux was high throughout the outburst, consistent with quasi-steady shell burning on the white dwarf. Given that accretion discs around white dwarfs with shell burning do not generally produce detectable X-rays (due to Compton-cooling of the boundary layer), the X-rays probably originated via shocks in the ejecta. As the X-ray photoelectric absorption did not vary significantly, the X-ray variability may directly link to the properties of the shocked material. AG Peg's transition from a slow symbiotic nova (which drove the 1850 outburst) to a classical symbiotic star suggests that shell burning in at least some symbiotic stars is residual burning from prior novae.

Key words: accretion, accretion discs – instabilities – binaries: symbiotic – stars: individual: AG Peg.

1 INTRODUCTION

Symbiotic Binaries have orbital periods with time-scales of years and contain a cool giant star which is losing mass, typically via a wind, to a hot compact star (see Allen 1984; Kenyon & Webbink 1984 and Mikołajewska 2007). The evolution of these systems has long been debated (e.g. Iben & Tutukov 1996), but there is now a growing appreciation that symbiotic binaries could produce some fraction of supernovae Ia outbursts (e.g. Di Stefano 2010; Dilday et al. 2012).

In their catalogue of symbiotic stars, Belczyński et al. (2000) list more than 200 known or suspected symbiotic stars, with more being discovered through surveys such as IPHAS (Corradi et al. 2008, 2010; Rodríguez-Flores et al. 2014). The optical photometric characteristics of symbiotic stars are diverse. Symbiotic stars can show 'classical' outbursts lasting weeks to years where they brighten by ∼1–2 mag. It is unclear if most of these outbursts are

due to nuclear burning on the surface of the white dwarf or an accretion disc instability of the sort seen in some cataclysmic variables (CVs) such as dwarf novae or a combination of both nuclear burning and a disc instability (as in Z And, Sokoloski et al. 2006). There are other symbiotic stars which show outbursts which are powered by thermonuclear runaways (TNRs), including slow novae where the outburst event can extend for many decades (e.g. Allen 1980; Kenyon & Truran 1983).

Observations made using the *Einstein* and *ROSAT* satellites showed that symbiotic stars are X-ray emitters at relatively low flux levels when in a quiescent state (Allen 1981; Mürset, Wolff & Jordan 1997). Luna et al. (2013) made a survey of symbiotic stars using the X-ray telescope (XRT) on-board the *Swift* satellite and found (as did Mürset et al. 1997) that they could group the sources into those which had very soft X-ray spectra (originating from shell burning on the surface of the white dwarf); those which had emission extending to ∼2.4 keV (probably due to the collision of winds from the red giant and white dwarf); and those which showed emission above ∼2.4 keV. Whereas Mürset et al. (1997) ascribed the hard X-rays to accretion on to a neutron star, Luna et al. (2013)

★ E-mail: gar@arm.ac.uk

attributed the thermal hard X-ray emission, as detected using the *Swift* XRT, to boundary layer emission around a white dwarf. Inevitably some sources showed X-ray spectra combining characteristics of more than one of these classes. These observations were generally made when the symbiotic binary had been in quiescence and not in outburst.

Most X-ray observations of symbiotic stars have typically been made at only one epoch. In contrast, observations of the symbiotic nova AG Dra made using *ROSAT* in 1994 show that the X-ray flux decreased over the course of the optical outburst (which was also noted in an earlier minor outburst using *EXOSAT* observations) which was attributed to the decrease in the temperature of the hot component, possibly due to an increase in the apparent size of its outer envelope (Greiner et al. 1997). An anti-correlation between the optical and X-ray flux over an outburst has also been seen in dwarf novae (e.g. Wheatley et al. 1996) and in the double degenerate interacting helium binary KL Dra (Ramsay et al. 2012).

The symbiotic binary AG Peg is one example of a slow symbiotic nova, which has a photometric record extending more than 200 yr. At the beginning of the 19th century AG Peg was recorded as a ~9.5 mag star which experienced a gradual brightening around 1850, reaching ~6 mag 20 yr later (Rigollet 1947; Belyakina 1968). (Mürset & Nussbaumer 1994, show the light curve of AG Peg extending over 150 yr.) Observations made by amateur astronomers whose records are accessible online (e.g. AAVSO[1] and BAAVSS[2]) date back to 1941. These show that AG Peg made a slow decline in brightness and only reached its pre 1850 outburst by the end of the 20th century. Indeed, there is evidence that the 1850 outburst was the slowest nova outburst ever recorded (e.g. Kenyon, Proga & Keyes 2001).

As AG Peg is a relatively bright object, it was studied spectroscopically by the end of the 19th century, showing a range of emission and absorption lines whose characteristics changed over months and decades. Later observations show the binary orbital period is 818.2 ± 1.6 d with an eccentricity of 0.11 (Merrill 1951; Fekel et al. 2000). The spectral type of the giant star is M3 III (Kenyon & Fernandez-Castro 1987), while the mass function of the system is consistent with the hot component being a white dwarf (Fekel et al. 2000).

There was some indication in 2013 May that AG Peg was beginning a new active phase when it was reported that AG Peg had brightend by ~0.3 mag (Munari et al. 2013). However, during June 2015 it was found that AG Peg had brightened from $V \sim 8.5$ to $V \sim 7.0$ over the course of a few weeks (Waagen 2015). Based on the long term light curve shown in Mürset & Nussbaumer (1994) and the records of the amateur astronomer groups mentioned earlier, we consider it highly unlikely that an outburst of the duration and amplitude of the 2015 outburst has taken place on AG Peg since the early 1940s, and the 2015 outburst is therefore likely to be the first bona fide outburst since the 19th century. However, we cannot exclude the possibility that a short duration event took place, for instance during the intervals when AG Peg was close to the Sun and therefore not observable.

We requested Target of Opportunity observations using *Swift* shortly after the announcement of the 2015 eruption and these observations showed that AG Peg was detected in X-rays during the optical outburst (Luna et al. 2015; Ramsay et al. 2015). Since these early observations, *Swift* has been used to observe AG Peg at regular
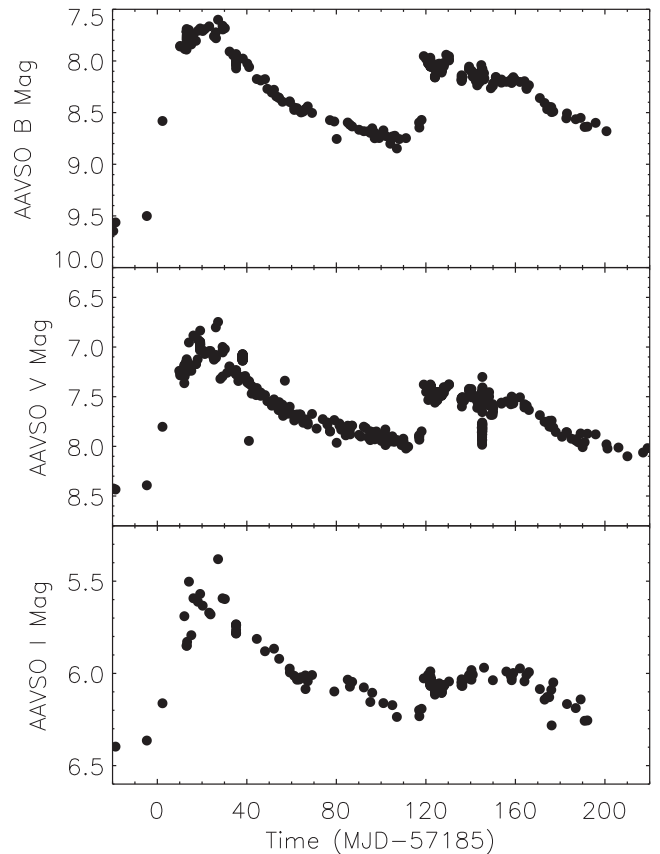
Figure 1. Photometry of AG Peg over the outburst in the *BVI* bands and taken from AAVSO data (Kafka 2015). We have not attempted to remove potentially discrepant data points. The outburst started on MJD=57185 which corresponds to 2015 June 12.

intervals. The main goal has been to determine how the X-ray flux (and spectrum) changes over the outburst and compare it with the observations of other accreting white dwarfs.

2 OVERVIEW OF OBSERVATIONS MADE BY AMATEUR OBSERVERS

2.1 Photometry

Observations made by amateur astronomers (e.g. AAVSO and BAA VSS) show that AG Peg was at $V \sim 8.5$ mag on 2015 June 6, reaching $V \sim 7.5$ by June 21 and reached a peak of $V \sim 6.8$ mag by the end of June (Fig. 1). Over the next 40 d it declined by half a magnitude after which it declined more slowly, reaching a plateau phase at $V \sim 7.8$ mag. Around October 10 AG Peg showed a 're-brightening' event reaching $V \sim 7.5$ mag after ~20 d, after which it started to decline. The peak magnitude of the June outburst was ~1 mag fainter than it was in 1870 and the rate of decline in this current outburst appears much quicker (e.g. Belyakina 1968). The amplitude of the outburst is higher in the *B* band (~1.8 mag) compared to the *I* band (~0.9 mag). These data also show the re-brightening event ($V \sim 0.5$ mag) occured on a time-scale of less than 1 d and was relatively brighter at bluer wavelengths compared to the 2015 June outburst.

2.2 Spectroscopy

AG Peg was observed using the LOTUS NUV-optical spectrograph on the Liverpool Telescope on 2015 July 1 (approximately 20 d after of the start of the outburst). Compared to pre-outburst spectra, the relative strength of O and N emission lines relative to the Balmer lines was stronger during the outburst (Steele et al. 2015).

Many groups, including amateur astronomers[3], have made spectroscopic observations of AG Peg over its outburst. These observations show strong emission lines, including the Balmer series plus He I (6678) and He II (4686), [O III] (4363) and the O VI emission band at 6825 Å, which is due to Raman scattering. A full analysis of the optical spectra made over the course of the outburst is beyond the scope of this work, but we were able to estimate the effective temperature of the ionizing source using the He II (4686) and H β lines and the formula of Iijima (1981) (quoted in Sokoloski et al. 2006) which derives the effective temperature using the equivalent width (EW) of these lines (we ignore the He I (4471) line since it is much weaker than He II and H β).

We used spectra taken by amateur astronomers[4] which covered the He II (4686) and H β lines to derive their EW (we estimated that the error on the EW measurements was ∼10 per cent by making a number of measurements of the same line). This shows that the EW of He II (4686) was somewhat variable over the outburst but showed a distinct decrease at the time of the optical re-brightening event (Fig. 2). This decrease is also seen in the EW of the H β line, although there is a trend for the EW to increase over the course of the outburst. We show the relative temperature over the course of the outburst in Fig. 2 which shows that the effective temperature of the ionizing source decreases over the duration of the outburst.

3 *SWIFT* OBSERVATIONS

3.1 Overview

The *Swift* satellite was launched in 2004 with a primary goal of detecting gamma-ray bursts, and locating and characterizing their X-ray and optical/UV properties (Gehrels et al. 2004). NASA runs a Target of Opportunity programme which provides the means for observing targets which have unexpectedly become interesting (novae for instance) at the earliest opportunity. Observations of AG Peg were made using *Swift* on 2015 June 28. Given the brightness of the source, it was saturated in the UVOT instrument (we discuss the implications of this in Section 4.3).

Because *Swift* is in a low Earth orbit, each observation sequence (which makes up an 'ObservationID') can be made up of more than one pointing, while the total exposure time of the X-ray observation in each ObservationID was typically 1–2 ks (see Table A1). The XRT (Burrows et al. 2005) on-board *Swift* has a field of view of 23.6×23.6 arcmin with CCD detectors allowing spectral information of X-ray sources to be determined. It is sensitive over the range 0.3–10 keV and at launch had a spectral resolution of 140 eV at 6 keV (which has since degraded over time).

The XRT has a number of modes of operation (designed to observe gamma-ray bursts at various stages of their evolution), but here we concentrate on the 'photon counting' mode which has full imaging and spectroscopic information. The data are processed us-
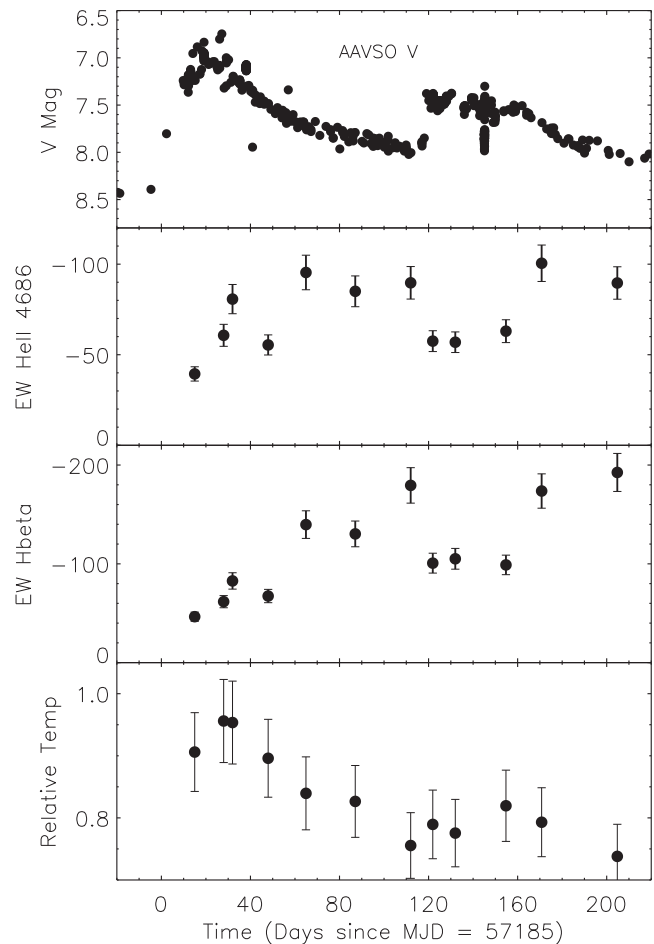

Figure 2. From the top we show the AAVSO *V*-band light curve; the equivalent width of the He II (4686) and H β line (derived using data taken by French amateur astronomers) and the relative effective temperature derived using these lines. As there is some uncertainty over the absolute temperature calibration using this method, we determine the relative temperature over the course of the outburst, where a value of unity implies an effective temperature of 1.9×10^5 K using the formula of Iijima (1981).

ing the standard XRT pipeline and it is these higher level products which we use in our analysis [5].

3.2 X-ray light curve

To determine the count rate of AG Peg at each epoch we filtered the X-ray events to extract photons with corresponding 'grades' 0–12 (this has the effect of filtering out events which are not from the target) and energy ranges from each ObservationID and made an image using `xselect`[6]. We used the HEASoft tool `XIMAGE` and the routine `SOSTA` (which takes into account effects such as vignetting, exposure and the point spread function) to determine the count rate and error at the position AG Peg. We determined an energy independent correction for each pointing to account for the fact that X-ray photons from AG Peg may have been deposited on known bad columns on the XRT detectors using the tool `xrtlccorr`[7].

---

[3] e.g. http://www.astronomie-amateur.fr
[4] http://www.astrosurf.com/aras/Aras_DataBase/Symbiotics/AGPeg.htm

[5] http://swift.gsfc.nasa.gov/docs/swift/analysis/xrt_swguide_v1_2.pdf
[6] http://heasarc.nasa.gov/docs/software/lheasoft/ftools/xselect/xselect.html
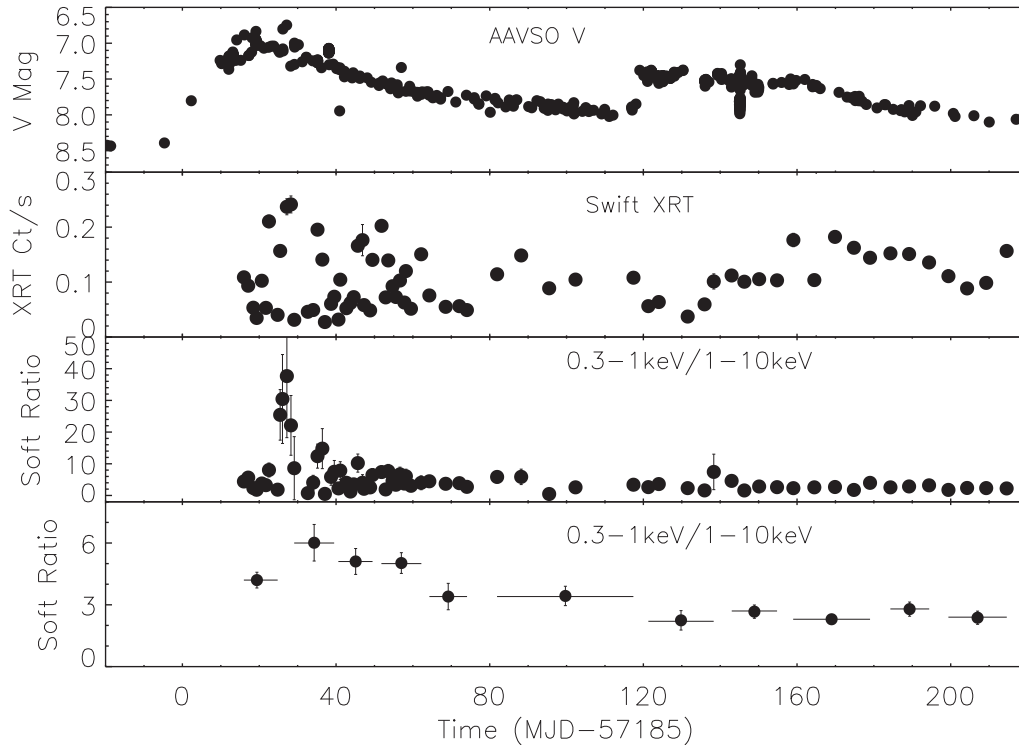[7] http://www.swift.ac.uk/analysis/xrt/lccorr.php

Figure 3. From the top we show: the *V* magnitude of AG Peg as obtained by AAVSO observers; the X-ray light curve of AG Peg (0.3–10 keV) as derived using *Swift* XRT data; the X-ray softness ratio; and the softness ratio where we have combined a number of epochs of data and (for clarity) we have omitted the epoch with the softest data points.

We show the count rate as a function of time since the start of the outburst in Fig. 3. (The characteristics of the X-ray light curve are very similar whether we apply the correction or not).

The first four epochs of the X-ray observations were made as AG Peg was just approaching maximum optical brightness and show a decreasing X-ray flux ($\sim$0.07 to 0.01 count s^{-1}). This compares with a count rate of 0.02–0.03 count s^{-1} when AG Peg was observed in 2013 Aug using the XRT. The X-ray flux then experiences some epochs of significantly enhanced X-ray rates reaching $\sim$0.3 count s^{-1} at MJD=57211 (26 d after the start of the outburst). As AG Peg slowly declines in optical flux the X-ray flux continues to show significant variations, although there is a decline in the peak count rate over this time interval.

As indicated earlier, approximately 120 d after the start of the optical outburst there is an optical rebrightening event where the system increases in brightness by $\sim$0.5 mag. In X-rays there is a decline in flux as the system brightens in the optical. However, by the time the system reaches maximum optical brightness and starts to decline, the X-ray flux starts to increase in flux, giving tentative evidence for a delay of $\sim$20 d between the X-ray and optical flux, or a suppression of X-rays during the rebrightening episode (Fig. 3).

To search for changes in the broad X-ray spectral distribution over the outburst we derived light curves (using the same method as before) for two energy bands: 0.3–1.0 keV and 1–10 keV (for reference we give the count rate in different energy bands in Table A1). We show how the softness ratio (0.3–1.0 keV/1–10 keV) changes over the outburst in Fig. 3. It is clear that during the time of highest flux (MJD$\sim$57210) the softness ratio is high (i.e. the spectrum is dominated by soft X-ray photons). As the source declines in optical flux, the large day-to-day X-ray flux variations are not reflected in changes to the softness ratio whose changes are much less marked. We also co-added data from different epochs to search for a

variation in the softness ratio as the outburst progressed and the results of this are shown in Fig. 3. The spectrum of AG Peg appears to harden after the very soft epoch reaching a minimum by the time of the onset of the rebrightening event. During the rebrightening event the softness ratio is roughly constant.

3.3 X-ray spectra

We now investigate the X-ray spectrum of AG Peg in more detail. Photons were extracted from a circular aperture centred on AG Peg and also a source-free region of the detector to create a background spectrum. We obtain an ancillary file, which allows us to determine the flux of the source, using an exposure map derived from the event files which are used to make up the spectrum. We used the response file, which allows the energy of each photon to be tagged, appropriate to the mode and grade of event, which was taken from the NASA HEASARC site[8]. The source spectrum was binned so that each bin had a minimum of 20 counts.

Using all the data, with the exception of the soft bright state, we obtain a spectrum with a total exposure time of 113.3 ks. This spectrum is consistent with that of absorbed thermal plasma emission with emission detected up to $\sim$3 keV. Mürset et al. (1997) and Luna et al. (2013) classed the X-ray properties of Symbiotic binaries according to the nature and energetics of the spectrum. The integrated spectrum of AG Peg during outburst is similar, for instance, to *Swift* J1719–3002 made during a quiescent state (Luna et al. 2013) which was classed as having a 'β' spectrum which indicates a spectrum peaking $\sim$0.8 keV, with most photons softer than 2.4 keV and is likely produced by a collision of winds from the white dwarf and

---

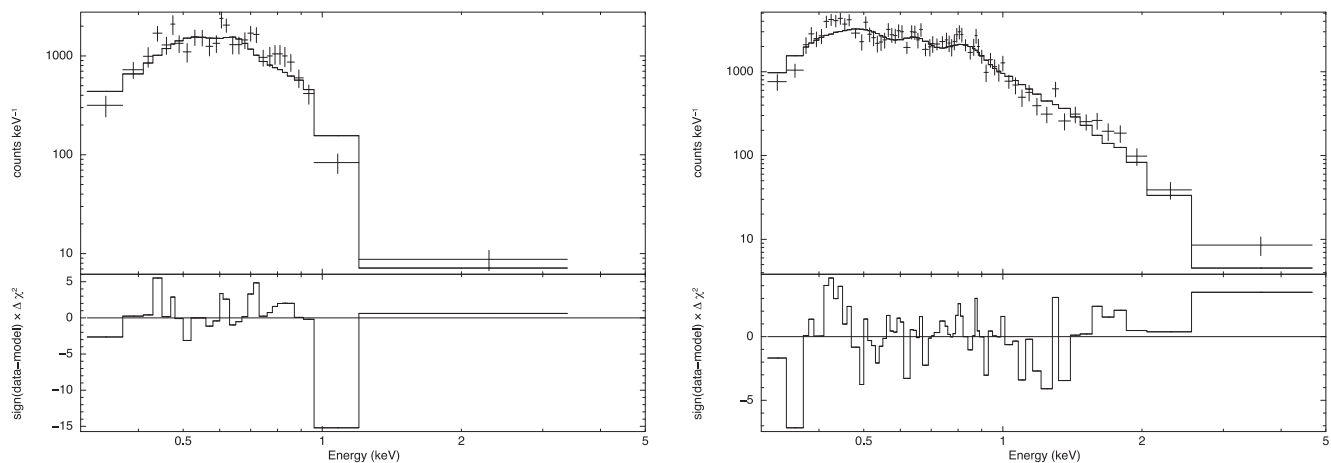[8] http://swift.gsfc.nasa.gov/proposals/swift_responses.html

Figure 4. On the left-hand side we show the X-ray spectrum taken during the soft X-ray phase and on the right the X-ray spectrum taken immediately after this (the 'high' phase). The model best fit is shown as a solid line and is an two temperature absorbed thermal plasma model.

red giant (∼1/3 of sources in the study of Luna et al. 2013 show a β type spectrum).

Using the X-ray fitting package XSPEC (Dorman & Arnaud 2001), we modelled the integrated spectrum using a range of emission models in combination with the tbabs absorption model (Wilms, Allen & McCray 2000). We found that although a two temperature thermal plasma model gave significantly better fits than a one temperature model it was not formally a good fit (χ_ν^2=2.60). We allowed various elements to have non-Solar abundances and whilst we obtained formally better fits, it was not a formally acceptable fit (χ_ν^2=1.59). In addition, there was some concern that we were obtaining non-physical abundances and therefore fitting noise in the spectrum.

The observed flux inferred from this model is 1.3×10^{-12} erg s^{-1} cm^{-2} (0.3–10 keV); the unabsorbed flux in the same band is 1.9×10^{-12} erg s^{-1} cm^{-2}, giving an X-ray luminosity, assuming a distance of 1 kpc (interferometric observations show AG Peg to have a parallax less than 1 mas, Boffin et al. 2014) of $L_X \sim 2.3 \times 10^{32}$ erg s^{-1} (which is typical for symbiotic stars in a quiescent state, c.f. Luna et al. 2013).

It is clear from the softness ratio shown in Fig. 3 that the X-ray spectrum is much softer ∼25 d after the start of the outburst. We extracted a spectrum from this soft phase and for comparison, we extracted a spectrum from data taken from pointings made in the next 30 d after this (the 'high' phase). We show the X-ray spectrum taken from the soft and high phases in Fig. 4. There is no evidence for a soft blackbody component in the 'soft' spectrum – rather the soft spectrum was best fit by a single thermal plasma model whilst the high spectrum was best fit using two thermal plasma models. The difference between the 'soft' and 'high' spectra was not due to different amounts of absorption. However, the goodness of fits to both spectra were still not formally acceptable (χ_ν^2=2.28 and χ_ν^2=1.63 for the soft and high spectra, respectively). We therefore do not provide additional details of the fits.

4 DISCUSSION

The 2015 outburst of AG Peg is the first to be observed since the mid 19th century. The duration and amplitude of these outbursts are very different in the optical, with the most recent being much shorter and of lower amplitude compared to the earlier outburst. We now discuss the physical reasons for these differences, the origin of the

X-ray emission, and the generation of quasi-steady nuclear burning on the white dwarfs in AG Peg and other symbiotic binaries.

4.1 The nature of the 2015 outburst

The 'slow-nova' outburst of AG Peg in the mid 19th century was almost certainly driven by a TNR on the surface of the accreting white dwarf (e.g. Gallagher et al. 1979; Kenyon et al. 1993). In contrast, the double-peaked 2015 outburst was much less energetic and of shorter duration. Moreover, whereas optical spectra taken during the decline of the slow-nova showed only absorption lines due to the expanded white dwarf photosphere (Gallagher et al. 1979), optical spectra during the 2015 eruption[9] displayed emission lines such as O VI (indicating highly ionized species in the nebula) which imply that material was still being exposed to the photoionizing hot white dwarf.

Rather than mimicking a slow-nova, the 2015 outburst appeared more similar to *classical* symbiotic outbursts which have time-scales of months to years (for instance Z And or AG Dra). The coverage of the optical photometry during the rise to optical maximum was not high enough to reveal whether the eruption was triggered by an accretion-disc instability, as in Z And. However, the optical light curve of Z And during the 2000–2002 event (shown in Sokoloski et al. 2006), also shows a rebrightening event and is remarkably like AG Peg, the difference being that in Z And the outburst lasted 2 yr rather than 6 months in the case of AG Peg. The re-brightening event is also reminiscent of brightness oscillations seen in classical symbiotic outbursts in e.g. CI Cyg, AX Per, and AG Dra (Mikołajewska & Kenyon 1992; Viotti et al. 2005), which some authors have speculated could be driven by resonances in an accretion disc. The modest increase in X-ray flux averaged over the 2015 event is also consistent with the increases in X-ray flux from Z And during its classical symbiotic outburst.

4.2 The origin of the X-ray emission

It is thought that classical outbursts from symbiotics may be driven by a disc instability, of the sort which drives dwarf nova outbursts, which can increase the rate of quasi-steady nuclear shell burning on

---

[9] e.g. http://www.astrosurf.com/aras/novae/InformationLetter/ARAS_EruptiveStars_2016-01.pdf

the white dwarf (Sokoloski et al. 2006). However, whereas almost all dwarf nova outbursts in CVs show a suppression of X-rays as the boundary layer between the accretion disc and the white dwarf becomes optically thick (with temperatures of just a few tens of eV; Wheatley et al. 1996), the connection between X-ray emission and the underlying physics is less clear in most classical symbiotic outbursts. In symbiotic stars with quasi-steady shell burning on the white dwarf, the accretion disc does not produce detectable X-ray emission because UV photons from the hot white dwarf Compton cool the boundary layer out of the X-ray regime (e.g. Luna et al. 2013). As discussed in Section 4.3, there is evidence that the white dwarf in AG Peg hosted shell burning throughout the 2015 eruption.

The temperature of the X-ray emission in AG Peg is much lower than the temperatures typically seen in dwarf novae in quiescence ($\sim$10 keV) – consistent with the idea that the X-ray emitting plasma in AG Peg was not located near the surface of the white dwarf, deep within its potential well. Our spectral models indicate temperatures below 1 keV. Super-soft X-ray emission is commonly seen after outbursts from novae and occasionally from symbiotics (e.g. AG Dra, Skopal et al. 2009). However, as expected for a low-mass white dwarf with quasi-steady shell burning, no super-soft X-ray emission was detected in AG Peg, confirming that nuclear burning did not lead to a white dwarf photosphere which was hot enough for blackbody emission to be seen in the supersoft X-rays.

One of the characteristics of the X-ray observations of AG Peg is the high day-to-day variability. X-ray observations of AG Peg started with *Swift* shortly before it reached peak optical brightness. They show that around 20–30 d after the optical peak, the X-ray emission became strongly variable on a time-scale shorter than a day and that the spectrum became soft for a handful of days. As AG Peg continued to fade in the optical, the X-ray flux continued to show day to day variations but the spectrum started to harden. At the time of the optical re-brightening event the X-ray flux reduced to very low levels until it started to increase after around 10 d. The degree of variability reduced and the hardness of the spectrum remained roughly constant.

Given that the level of absorption did not show an overall decrease over the course of the outburst – as one might expect for the clearing of ejecta – we do not find evidence that the day-to-day variability was due to changing levels of absorption from a clumpy outflow. However, we do expect that shocks were generated in the AG Peg outburst as ejecta interacted with circumbinary material (see e.g. Mürset, Wolff & Jordan 1977; Pan, Ricker & Taam 2015). In an extreme case of such interactions, the 2006 outburst of RS Oph triggered a shock wave that was seen at multiple wavelengths (e.g. O'Brien et al. 2006). In the 2000–2002 outburst of Z And, a jet was seen at radio wavelengths (Brocksopp et al. 2004), and it is known that jets from symbiotic binaries can produce faint X-rays (e.g. Galloway & Sokoloski 2004; Karovska et al. 2007, 2010; Kellogg et al. 2007; Nichols et al. 2007). Evidence for winds in symbiotic binaries, including AG Peg (Nussbaumer, Schmutz & Vogel 1995), is widespread. The optical spectra discussed in Section 2.2 show evidence for extended wing features in the Balmer line emission during the 2015 outburst. For X-ray temperatures <1keV, we would expect shock speeds slower than 1000 km s^{-1} (see equation 4 of Stute, Luna & Sokoloski 2011), consistent with the optical line widths. Taking a Bremsstrahlung cooling time of:

$$t_{\mathrm{Bremss}} = \left(\frac{T}{2} \times 10^6 \mathrm{K} \right)^{1/2} \left(\frac{n}{3} \times 10^9 \mathrm{cm}^{-3} \right) \sim \mathrm{d} \qquad (1)$$

(Frank, King & Raine 2002), the rapid X-ray variability suggests that the shocked gas was probably quite dense. Alternatively, if the

rapid variability was due to adiabatic-expansion cooling of shocked clumps, the clumps must have been less than $\sim$10^{12} cm (or $\sim$1/10 of an au) in size. High densities and small clump sizes are both plausible, so the rapid X-ray variability is consistent with our hypothesis that the X-ray emission was due to shocks associated with a (perhaps collimated) eruptive outflow.

Approximately 120 d after the start of the outburst, the optical flux brightened by $V \sim 0.5$ mag in less than a day, after which it showed a gradual decline over $\sim$40 d followed by a more rapid decline. A rebrightening event was also seen in the 2000–2002 outburst of Z And which was attributed to a decrease in the temperature of the optical emitting material due to a slight expansion of the white dwarf photosphere (Sokoloski et al. 2006). However, the temperature derived from the He II and H β lines (Fig. 2) suggest the temperature did not change significantly over the course of the rebrightening event. The *Swift* observations of AG Peg show a suggestion of a $\sim$20 d delay between the initial rise of the optical and X-ray fluxes at this epoch.

Compared to dwarf nova outbursts, symbiotic binaries show a greater diversity of X-ray/optical characteristics over an outburst cycle. AG Dra, whose 1994–1995 outburst was driven by an expansion of the photosphere of the shell-burning white dwarf, showed a clear drop in X-ray flux (0.1–2.4 keV) during an optical outburst (Greiner et al. 1997). On the other hand the symbiotic star V407 Cyg shows an *increase* in the 0.3–10 keV flux around 20 d after an outburst in 2010 in which ejecta collided with circumbinary material (Nelson et al. 2012). Based on the similarity between the optical light curves of AG Peg and Z And, we suggest that the 2015 outburst of AG Peg was also triggered by an accretion instability. Based on the properties of the X-ray emission, we suggest that enough material was ejected during the outburst to heat ejecta and/or circumbinary material through shocks.

4.3 Origin of quasi-steady shell burning in classical symbiotic stars

Mürset et al. (1991) and Skopal (2005) modelled UV spectra of a sample of symbiotic stars obtained using *IUE* and found white dwarf temperatures and luminosities around $\sim$10^5 K and $\sim$10^3 L$_\odot$, respectively — much higher than expected from accretion alone. Because nuclear burning releases 40 to 50 times more energy per nucleon than accretion on to a white dwarf, these high temperatures and luminosities are naturally explained if shell burning is present. Given that shell burning is not a common (long-term) feature of accreting white dwarfs in CVs, why is it so frequently present in symbiotic stars?

Two main possibilities exist for the origin of quasi-steady shell burning in normal white dwarf symbiotics. It could be the result of accretion at a rate above the theoretical minimum for shell burning but below the value that leads to expansion of the white dwarf envelope to giant dimensions (Paczyński & Żytkow 1978; Sion, Acierno & Tomczyk 1979; Paczyński & Rudak 1980; Iben 1982; Fujimoto 1982a; Nomoto 1982a,b). One problem with this scenario, however, is that the range of accretion rates that produce steady burning is narrow (a factor of a few, Fujimoto 1982b), and it seems unlikely that most symbiotic stars accrete at a rate just within this range. The other alternative is that the observed quasi-steady shell burning is residual burning from a prior nova.

The lower limits that *Swift*/UVOT placed on the UV flux during the 2015 event attest to the continued presence of shell burning on the surface of the white dwarf while it experienced classical symbiotic eruptions. The *Swift*/UVOT saturates through the *UVW*2 filter at

around 12.6 mag (in the AB system[10]), which corresponds to a flux density at 1928 Å of 2.75×10^{-13} erg s^{-1} cm^{-2} Å^{-1}. Multiplying this value by the UVW2 filter width of 657 Å (Poole et al. 2008), dereddening it using the $E(B-V)=0.1$ (Kenyon et al. 1993), and taking a distance of at least 1 kpc (Boffin et al. 2014), we find a luminosity between approximately 1600 Å and 2260 Å of at least 4.3×10^{34} erg s^{-1}. The presence of the Raman-scattered O VI line (at 6825 Å) throughout the 2015 eruption indicates that the temperature of the hot white dwarf remained above 110 000 K (Mürset & Nussbaumer 1994). We therefore multiply the 1600–2260 Å luminosity by a factor of 5 as a conservative bolometric correction (for a white dwarf that either hosts shell burning or accretes at a very high rate). Keeping in mind that both the UVOT flux and the distance are lower limits, we conclude that the luminosity of either the white dwarf or the accretion disc was likely well in excess of $\sim 2 \times 10^{35}$ erg s^{-1} during the recent outburst.

For the disc to have produced this luminosity it would have required an accretion rate above $\sim 10^{-7}$ M$_\odot$ yr^{-1}. It is theoretically challenging, however, for a 0.6 M$_\odot$ white dwarf to accrete at such a high rate without generating quasi-steady shell burning (Paczyński & Żytkow 1978; Nomoto 1982a). As in other classical symbiotic stars, such as Z And and AG Dra, the most natural interpretation is that quasi-steady shell burning remains present on the surface of the white dwarf.

AG Peg's transition from a slow nova to a classical symbiotic, marked by classical symbiotic outbursts, suggests that shell burning in at least some (and perhaps most) symbiotics with strong optical emission lines is residual burning from prior novae outbursts. That the luminosity of the white dwarf in AG Peg was very low before the 19th century slow nova (Mürset & Nussbaumer 1994) confirms that material was not burning on the white dwarf before that event. After the start of the slow nova, however, the temperature and luminosity were consistently high enough to indicate shell burning (Mürset & Nussbaumer 1994). In fact, the slow nova led to a prolonged period of burning that persisted through the recent active phase. The lack of any hard X-ray emission from the accretion-disc boundary layer in 2013 (despite AG Peg's distance of only about 1 kpc and its exteme UV brightness; Nuñez & Luna 2013) supports the notion that shell burning was present through 2013.

As we argued above, the continued UV brightness throughout the recent period of optical activity implies that shell burning is ongoing. Interestingly, RX Pup, which has been identified as a symbiotic slow nova by Mikołajewska et al. (2002), also experienced an optical rebrightening. If the steady burning in other symbiotic stars is also the result of prior novae, it would follow that accretion on to the white dwarf in these systems does not necessarily proceed at the rate required for quasi-steady shell burning. Shell burning arising from prior novae would also have implications for selection biases in the sample of known symbiotic stars and the efficiency with which symbiotic white dwarfs can retain accreted material.

5 SUMMARY AND CONCLUSIONS

The optical outburst of AG Peg in 2015 had a lower amplitude and much shorter duration than the outburst observed in the mid 19th century. The earlier event was very likely driven by a TNR on the surface of the white dwarf. In contrast, the recent event is similar to classical symbiotic outbursts in which an accretion instability dumps fuel on to an already burning white dwarf. The

optical light curve of AG Peg is very similar (if taking place over a shorter time-scale) to the 2000–2002 outburst of Z And. The X-ray observations show strong soft X-ray emission which has large day-to-day variations 20–30 d after outburst. The X-ray flux continued to show marked day-to-day variations for another month. This variability is similar to that seen in some novae such as RS Oph which is thought to be due to shocks interacting with clumpy material in the ejecta and emitting X-rays. There is also evidence that the optical rebrightening event showed X-rays being delayed by ∼20 d compared to the optical, hinting that material had to clear in order for the X-rays to be seen. Irrespective of the exact causes of the 2015 outburst of AG Peg and its X-ray emission, it is clear that AG Peg has stopped behaving like a slow nova and started behaving like a classical symbiotic star. With this transition, AG Peg provides support for the idea that quasi-steady shell burning on the white dwarfs in symbiotic stars is residual burning from prior novae.

REFERENCES

Allen D. A., 1980, MNRAS, 192, 521
Allen D. A., 1981, MNRAS, 197, 739
Allen D. A., 1984, Ap&SS, 99, 101
Belczyński K., Mikołajewska J., Munari U., Ivison R. J., Friedjung M., 2000, A&AS, 146, 407
Belyakina T. S., 1968, SvA, 110
Boffin H. M. J., Hillen M., Berger J. P., Jorissen A., Blind N., Le Bouquin J. B., Mikołajewska J., Lazareff B., 2014, A&A, 564, 1
Brocksopp C., Sokoloski J. L., Kaiser C., Richards A. M., Muxlow T. W. B., Seymour N., 2004, MNRAS, 347, 430
Burrows D. N. et al., 2005, Space Sci. Rev., 120, 165
Corradi R. L. M. et al., 2008, A&A, 480, 409
Corradi R. L. M. et al., 2010, A&A, 509, 41
Di Stefano R., 2010, ApJ, 719, 474
Dilday B. et al., 2012, Science, 337, 942
Dorman B., Arnaud K. A., 2001, in Harnden F. R., Jr, Primini F. A., Payne H. E., eds, ASP Conf. Ser. Vol. 238, Astronomical Data Analysis Software and Systems X. Astron. Soc. Pac., San Francisco, p. 415
Fekel F. C., Joyce R. R., Hinkle K. H., Skrutkie M. F., 2000, AJ, 19, 1375
Frank J., King A., Raine D. J., 2002, Accretion Power in Astrophysics. Cambridge Univ. Press, Cambridge
Fujimoto M. Y., 1982a, ApJ, 257, 752
Fujimoto M. Y., 1982b, ApJ, 257, 767
Gallagher J. S., Webbink R. F., Holm A. V., Anderson C. M., 1979, ApJ, 229, 994
Galloway D. K., Sokoloski J. L., 2004, ApJ, 613, L61
Gehrels N. et al., 2004, ApJ, 611, 1005

[10] http://swift.gsfc.nasa.gov/analysis/uvot_digest/coiloss.html

G. Ramsay et al.

Greiner J., Bickert K., Luthardt R., Viotti R., Altamore A., Gonzalez-Riestra R., Stencel R. E., 1997, A&A, 322, 576

Iben I., 1982, ApJ, 259, 244

Iben I., Tutukov A. V., 1996, ApJS, 105, 145

Iijima T., 1981, in Carling E. B., Kopal Z., eds, Photometric and Spectroscopic Binary Systems. Dordrecht, Kluwer, p. 517

Kafka S., 2015, Observations from the AAVSO International Database. Available at: http://www.aavso.org.

Karovska M., Carilli C. L., Raymond J. C., Mattei J. A., 2007, ApJ, 661, 1048

Karovska M., Gaetz T. J., Carilli C. L., Hack W., Raymond J. C., Lee N. P., 2010, ApJ, 710, L132

Kellogg E., Anderson C., Korreck K., DePasquale J., Nichols J., Sokoloski J. L., Krauss M., Pedelty J., 2007, ApJ, 664, 1079

Kenyon S. J., Fernandez-Castro T., 1987, AJ, 93, 938

Kenyon S. J., Truran J. W., 1983, ApJ, 273, 280

Kenyon S. J., Webbink R. F., 1984, ApJ, 279, 252

Kenyon S. J., Mikołajewska J., Mikołajewski M., Polidan R. S., Slovak M. H., 1993, AJ, 106, 1573

Kenyon S. J., Proga D., Keyes C. D., 2001, AJ, 122, 349

Luna G. J. M., Sokoloski L. J., Mukai K., Nelson T., 2013, A&A, 559, 6

Luna G. J. M., Nuñez E. N., Sokoloski L. J., Montane B., 2015, Astron. Telegram, 7741

Merrill P. W., 1951, ApJ, 113, 605

Mikołajewska J., 2007, Balt. Astron., 16, 1

Mikołajewska J., Kenyon S., 1992, MNRAS, 256, 177

Mikołajewska J., Brandi E., Garcia L., Ferrer O., Quiroga C., Anupama G. C., 2002, in Hernanz M., Jose J., eds, Proc. AIP Conf. Vol. 637, Classical Novae Explosions, New York, p. 42

Munari U., Valisa P., Dallaporta S., Cherini G., Righetti G. L., Castellani F., 2013, Astron. Telegram 5258

Mürset U., Nussbaumer H., 1994, A&A, 282, 586

Mürset U., Nussbaumer H., Schmid H. M., Vogel M., 1991, A&A, 248, 458

Mürset U., Wolff B., Jordan S., 1997, A&A, 319, 201

Nelson T., Donato D., Mukai K., Sokoloski J., Chomiuk L., 2012, ApJ, 74, 43

Nichols J. S., DePasquale J., Kellogg E., Anderson C. S., Sokoloski J., Pedelty J., 2007, ApJ, 660, 651

Nomoto K., 1982a, ApJ, 253, 798

Nomoto K., 1982b, ApJ, 257, 780

Nuñez N. E., Luna G. J. M., 2013, Astron. Telegram, 5324

Nussbaumer H., Schmutz W., Vogel M., 1995, A&A, 293, L13

O'Brien T. et al., 2006, Nature, 442, 279

Paczyński B., Rudak B., 1980, A&A, 82, 349

Paczyński B., Żytkow A. N., 1978, ApJ, 222, 604

Pan K.-C., Ricker P. M., Taam R. E., 2015, ApJ, 806, 27

Poole T. S. et al., 2008, MNRAS, 383, 627

Ramsay G., Wheatley P. J., Rosen S., Barclay T., Steeghs D., 2012, MNRAS, 425, 1486

Ramsay G., Luna G. J. M., Nuñez E. N., Sokoloski L. J., Montane B., 2015, Astron. Telegram, 7779

Rigollet R., 1947, L'Astronomie, 61, 54

Rodríguez-Flores E. R. et al., 2014, A&A, 567, 49

Sion E. M., Acierno M. J., Tomczyk S., 1979, ApJ, 230, 832

Skopal A., 2005, A&A, 440, 995

Skopal A., Sekeráš M., González-Riestra R., Viotti R. F., 2009, A&A, 507, 1531

Sokoloski J. L. et al., 2006, ApJ, 636, 1002

Steele I. A., Jermak H. E., Marchant J. M., Bates S. D., 2015, Astron. Telegram, 7749

Stute M., Luna G. J. M., Sokoloski J. L., 2011, ApJ, 731, 12

Viotti R. et al., 2005, Ap&SS, 296, 435

Waagen E. O., 2015, AAVSO Alert Notice 521

Wheatley P. J., Verbunt F., Belloni T., Watson M. G., Naylor T., Ishida M., Duck S. R., Pfeffermann E., 1996, A&A, 307, 137

Wilms J., Allen A., McCray R., 2000, ApJ, 542, 914

SUPPORTING INFORMATION

Additional Supporting Information may be found in the online version of this article:

Table A1. The observation log for the *Swift* XRT observations. We indicate the Observation ID (ObsID); the start of the observations; the time since the optical outburst (defined as MJD=57185 = 2015 June 12); the duration of the XRT exposure and then the observed count rate and error (1σ) in the 0.3–10 keV, 0.3–1 keV and 1–10 keV energy bands. We have applied a correction to take into account that some fraction of the source PSF make have overlapped with dead columns on the detector (see text for details). (http://www.mnras.oxfordjournals.org/lookup/suppl/doi:10.1093/mnras/stw1546/-/DC1).

Please note: Oxford University Press is not responsible for the content or functionality of any supporting materials supplied by the authors. Any queries (other than missing material) should be directed to the corresponding author for the paper.

APPENDIX A: TABLE

Table A1. The observation log for the *Swift* XRT observations. We indicate the Observation ID (ObsID); the start of the observations; the time since the optical outburst (defined as MJD=57185 = 2015 June 12); the duration of the XRT exposure and then the observed count rate and error (1σ) in the 0.3–10 keV, 0.3–1 keV and 1–10 keV energy bands. We have applied a correction to take into account that some fraction of the source PSF make have overlapped with dead columns on the detector (see text for details).

ObsID	Start time (MJD)	Time from Outburst (d)	XRT exp (s)	0.3–10 keV (Ct s^{-1})	±	0.3-1 keV (Ct s^{-1})	±	1–10 keV (Ct s^{-1})	±
00032906003	57201.017	16.0	8949	0.1140	0.0045	0.0868	0.0040	0.0197	0.0019
00032906004	57202.128	17.1	1923	0.0951	0.0078	0.0809	0.0072	0.0143	0.0030
00032906005	57203.466	18.5	1627	0.0457	0.0006	0.0321	0.0050	0.0136	0.0033
00032906006	57204.324	19.3	1555	0.0227	0.0044	0.0143	0.0034	0.0080	0.0025
00032906007	57205.667	20.7	1916	0.1063	0.0086	0.0791	0.0074	0.0209	0.0038
00032906008	57206.735	21.7	2018	0.0454	0.0047	0.0392	0.0044	0.0121	0.0025
00032906009	57207.535	22.5	1419	0.2395	0.0140	0.2144	0.0140	0.0267	0.0048
00032906011	57209.784	24.8	1978	0.0297	0.0036	0.0203	0.0030	0.0111	0.0022
00032906012	57210.450	25.4	4864	0.1732	0.0062	0.1620	0.0060	0.0064	0.0012
00032906013	57211.055	26.1	903	0.3954	0.0250	0.3803	0.0240	0.0125	0.0044
. . .	. . .	. . .	. . .	. . .	. . .	. . .	. . .	. . .	. . .

This paper has been typeset from a TEX/LATEX file prepared by the author.

Downloaded from https://academic.oup.com/mnras/article-abstract/461/4/3599/2608617 by guest on 25 November 2019